Available online at www.sciencedirect.com
SCIENCE DIRECT®
Pergamon
Acta Materialia 51 (2003) 207–216
Acta MATERIALIA
www.actamat-journals.com

Application of the cluster-site approximation (CSA) model to the f.c.c. phase in the Ni–Al system

F. Zhang [a,*], Y.A. Chang [b], Y. Du [b], S.-L. Chen [a], W.A. Oates [c]

[a] *CompuTherm LLC, 437 S. Yellowstone Dr., Madison, WI 53719, USA*
[b] *Department of Materials Science and Engineering, University of Wisconsin-Madison, Madison, WI 53706, USA*
[c] *Science Research Institute, University of Salford, Salford M5 4WT, UK*

Received 20 May 2002; accepted 16 August 2002

Abstract

The modified cluster-site approximation (CSA) model has been used to model the f.c.c. phases (ordered $L1_2$ and disordered $A1$) in the Ni–Al system. The CSA model has the advantage over the cluster variation method (CVM) in that the independent variables in the free energy functional are the site probabilities and not the cluster probabilities. Unlike the zeroth approximation, however, the CSA takes short-range order into consideration, an essential requirement for describing phases that undergo an order/disorder transition, as does the f.c.c. phase in the Ni–Al system. By using the modified CSA model, we have been able to obtain an improved phenomenological description of this system with the use of fewer model parameters than used in previous descriptions. The topology of the calculated metastable f.c.c. phase diagram is similar to the one obtained using a 'first-principles'-CVM approach, whereas the f.c.c. phase diagrams based on the previous phenomenological descriptions are unsatisfactory.

Keywords: Cluster-site approximation; Nickel alloys; Phase diagrams; Order-disorder phenomena; Thermodynamics

1. Introduction

The thermodynamics and phase diagram of the Ni–Al binary system have been studied in great detail because of the importance of this system for understanding the behavior of Ni-based superalloys. In addition to a large experimental effort, several versions of the calculated Ni–Al phase diagram have been published [1–6]. In these calculations, the energy parameters were obtained by either a phenomenological approach [1–4], or a 'first principles' approach [5,6]. The entropies of mixing were calculated by using either the zeroth approximation [1–3], often referred to as Bragg-Williams approximation [7,8], or a higher order approximation [4–6], namely, the Cluster Variation Method (CVM) [9].

The most recent thermodynamic description by Huang and Chang [3] was quite successful when judged by the small number of parameters used and the good agreement with the experimental data. However, they described the two states of the f.c.c. phase as two separate phases, i.e., γ for the disordered state ($A1$), and γ' for the ordered state

* Corresponding author.
E-mail address: fan@chorus.net (F. Zhang).

1359-6454/03/$22.00
doi:10.1016/S1359-6454(02)00392-0

($L1_2$). The γ phase was modeled using a substitutional solution model, while a two sublattice compound energy model [10] was used for the γ' phase. The compound energy model uses the zeroth approximation to evaluate the entropy of mixing, even though it is well known that this approximation is not suitable for describing order/disorder transitions, such as the γ'/γ transition in the Ni–Al system, due to its neglect of short-range order. Ansara et al. [2], on the other hand, modeled both γ and γ' as one phase using a two sublattice compound energy model. Because of the inherent weakness of the model, however, Ansara et al. [2] had to use many adjustable parameters for the liquid and f.c.c. phases in order to fit the experimental data.

The CVM, which takes short-range order into consideration, has been applied to the Ni–Al system [4–6]. Sigli and Sanchez [4] optimized the energy parameters using experimental data, whilst Pasturel et al. [5] and Lechermann et al. [6] obtained the cluster energy parameters from 'first principles' calculations.

Although the CVM is much better in describing order/disorder transitions than the zeroth approximation, its application to multicomponent phase diagram calculations is rather limited because of the large number of non-linear equations which must be solved simultaneously to obtain the free energy and the equilibrium species distribution, viz., in the order of C^n, with C being the number of components and n being the size of the cluster, e.g., 10000 for a 10 component system and using a tetrahedron cluster. Because of this, its application to technologically important systems, which often contain more than 10 components, seems impractical. It should also be remarked that the Ni–Al phase diagrams calculated by Sigli and Sanchez [4], Pasturel et al. [5], and Lechermann et al. [6] are only qualitatively correct; they lack the accuracy for practical applications. This is because other, non-configurational, contributions to the high temperature free energy were not accounted for with the necessary accuracy.

Although not as physically sound as the CVM, the Cluster-Site Approximation (CSA) has the considerable advantage of computational simplicity over the CVM [11]. Its superiority in regard to multicomponent phase diagram calculations was pointed out by Oates and Wenzl [12], although the crucial result used is clearly recognizable in the work of Fowler [13] and Yang and Li [14–17]. This is that the free energy can be expressed in terms of the site probabilities only instead of the cluster probabilities as in the CVM. The effect of this is to drastically reduce the number of independent variables in the free energy functional. The number of equations need to be solved in the CSA is in the order of $C \times n$, instead of the C^n required in the CVM because the independent variables are the site probabilities, as in the zeroth approximation, instead of the cluster probabilities. Moreover, unlike the zeroth approximation, the CSA takes short-range order into consideration and is thus suitable for describing order/disorder transitions. The CSA method has been discussed elsewhere and has been successfully applied to the Au–Cu, Au–Ni, and Cd–Mg systems [11,12,18,19]. In the present paper, we show how the CSA model can be applied successfully to describe the different coherent states of the f.c.c. phase in the Ni–Al system.

2. The cluster-site approximation (CSA)

The CSA is an adaptation of the generalized quasi-chemical method, introduced many years ago by Fowler for treating atom/molecule equilibria in gases [13] and subsequently used for clusters in solid solutions by Yang and Li [14–17]. The unique feature of the CSA is that the clusters are energetically non-interfering, i.e., they are allowed to share only sites at the cluster corners. This cluster non-interference always results in a two-term expression for the configurational entropy, irrespective of the cluster size. In the original Yang and Li's calculations [14–17], the two-term expression for the entropy per site S_m was written as

$$S_m = \frac{z}{2p}S_n - \left(\frac{nz}{2p} - 1\right)S_1 \tag{1}$$

where $z/2p$ is the number of non-interfering clusters per site, z being the nearest-neighbor coordination number of the lattice and p the number of nearest-neighbor pairs in the cluster of size n. The

S_n and S_1 are the cluster and point entropies, respectively, defined as $S_n = -k\sum_i p_i \ln(p_i)$, where p_i is the cluster (or site) probability of type i.

It can be seen that Eq. (1) is correct in the high temperature limit where $S_m \rightarrow S_1$. The entropy expression from the CSA is simpler than that obtained from the CVM [9] in that the sub-clusters (cluster edges, surfaces etc.) are not involved in the calculation because of the non-interference of clusters approximation.

In the CSA, the molar free energy F_m for a binary system A–B is given by [11]:

$$\frac{F_m}{RT} = \frac{z}{2p}\left(\sum_{i=1}^{n}(y_A^i\mu_A^i - \ln\varphi)\right) - \left(\frac{nz}{2p} - 1\right)\sum_{i=1}^{n}\sum_{q=A,B} f_i y_q^i \ln y_q^i \quad (2)$$

where the f_i is the fraction of sublattices of type i and the y_q^i is the species concentration of component q on sublattice i. The μ_A^is are Lagrangian multipliers associated with atom balances and, physically, are related to the species chemical potentials of the equivalent lattice gas particles on sublattice i.

The cluster partition function, φ, is given by:

$$\varphi = \sum_{j=1}^{2^n} \exp\left[\left(\sum_{i=1}^{n}\mu_A^i\right)_j - \varepsilon_j\right] \quad (3)$$

where ε_j is the cluster energy of a j-type cluster.

The original cluster-site approximation proposed by Yang and Li [14–17] fell into disuse shortly after its introduction because it was quickly superceded by the more accurate CVM [9]. But it has been demonstrated [11] that the CSA can be made more versatile in phenomenological phase diagram calculations by introducing a simple modification to Eq. (2) and also by splitting the Gibbs energy of a phase into configuration-dependent (CSA) and configuration-independent contributions [20]. The modified CSA equation for the Gibbs energy of mixing, for a binary A–B alloy when a cluster containing n atoms is used, is then given by:

$$\Delta G^M = \xi\Delta G_n - (n\xi - 1)\Delta G_1 + G_{CI}^E(x,T) \quad (4)$$

The first two terms on the right side of the equation are from Eq. (2) with

$$\Delta G_n = RT\left(\sum_{i=1}^{n} y_A^i\mu_A^i - \ln\varphi\right) \quad (5)$$

$$\Delta G_1 = RT\sum_{i=1}^{n}\sum_{q=A,B} f_i y_q^i \ln y_q^i \quad (6)$$

$$\xi = \frac{z}{2p} \quad (7)$$

The number of non-interfering clusters per site, $z/2p$, in the original CSA model is substituted by the factor ξ which is an adjustable parameter, with a value not too different from $z/2p$. Although the adjustment to the mixing entropy brought about by this modification is quite small, it is critical in making the CSA model applicable to real alloy systems. The third term on the right-hand side of Eq. (4) is the configuration independent term (one which depends on molar composition, x, only and not on the details of sublattice occupation). It is used to take into account elastic energies due to atomic size mismatch or changing cell relaxation and also any excess excitation contributions. In a phenomenological calculation it can be expressed as a Redlich–Kister polynomial [21] of composition x, and temperature T, with coefficients L being the model parameters:

$$G_{CI}^E(x,T) = x(1-x)\sum_{m=0}(1-2x)^m\sum_{\nu=0} L_\nu^{(m)}T^\nu \quad (8)$$

ΔG^M in Eq. (4) is thus a functional of the geometrical factor ξ in Eq. (7), the composition x, temperature T, and the y_A^is in Eqs. (5) and (6). The geometrical factor, the cluster energy parameters and the L parameters are the model parameters whose values are optimized using experimental data. When the model parameters are obtained in this way, the equilibrium species distributions (y_A^is) can be obtained as a function of temperature and composition by minimizing the Gibbs energy defined by Eq. (4). Note that the μ_A^is in Eq. (5), being species chemical potentials, are uniquely related to the y_A^is, so that either can be used as variables in the minimization.

The modified CSA has significant advantages

over the CVM in phenomenological calculations of phase diagrams:

1. By using energetically non-interfering clusters, the number of independent variables in the free energy functional is changed from being the cluster probabilities in the CVM to being the point probabilities in the CSA, e.g., from 10^4 to 10x4 for a 10 component system with a tetrahedron cluster. This large reduction in the number of variables makes the CSA attractive for application to multicomponent alloys [12].
2. By using ξ as an adjustable parameter and incorporating the configuration independent term, more flexibility is obtained in describing the Gibbs energy-composition curves. This point was illustrated in the calculation of the Au–Cu ordering phase diagram [11].

On the other hand, the modified CSA also has advantages over the zeroth approximation in describing phases undergoing order/disorder transitions in that it takes short-range order into consideration. Even though the Gibbs energy of a phase in the CSA model is described as a function of point probabilities, the cluster probabilities can be calculated explicitly as follows:

$$p_{jkl\ldots} = \frac{\mu_j^I \cdot \mu_k^{II} \cdot \mu_l^{III} \ldots}{\varphi} \cdot \exp(-\varepsilon_{jkl\ldots}) \tag{9}$$

where $p_{jkl}\ldots$ is the probability of forming *jkl* type of cluster, $\varepsilon_{jkl\ldots}$ the energy of such a cluster, and φ is defined in Eq. (3). The μ_q^is are defined as:

$$\begin{cases} \mu_q^i = \mu_A^i & \text{if } q = A \\ \mu_q^i = 1 & \text{if } q = B \end{cases} \tag{10}$$

their values are obtained by the minimization of the Gibbs energy defined in Eq. (4). Similarly, the probability of a sub-cluster can also be calculated using the probabilities of the corresponding clusters. For example,

$$p_{ijk} = \sum_{l=A,B} p_{ijkl} \tag{11}$$

3. Application of the CSA to the Ni–Al system

The phases considered in the Ni–Al system are: liquid, Al_3Ni, Al_3Ni_5, B2–NiAl, Al_3Ni_2, and f.c.c.. The f.c.c. phase is present in two stable states in this binary system, i.e., the disordered state ($A1$), represented by γ in the stable phase diagram, and the ordered state ($L1_2$), represented by γ'. Since the principal purpose of the present study was to explore the use of the modified CSA for describing an order/disorder transition in a real alloy system, only the f.c.c. phase has been described by the CSA model. The thermodynamic models normally used in phenomenological modeling, as used by Huang and Chang [3] in this particular case, have been used to describe the other five phases.

To describe the f.c.c. structure, the nearest neighbor tetrahedron cluster, shown in Fig. 1, was chosen in this study. The cluster size is thus four, and a total of 16 different types of tetrahedron clusters are possible in a binary system. This means a total of 16 energy parameters are needed in the calculation. In order to reduce the number of cluster energies involved, we have related the cluster energies to the nearest neighbor pair interaction energies. From Fig. 1, the following relations are obtained:

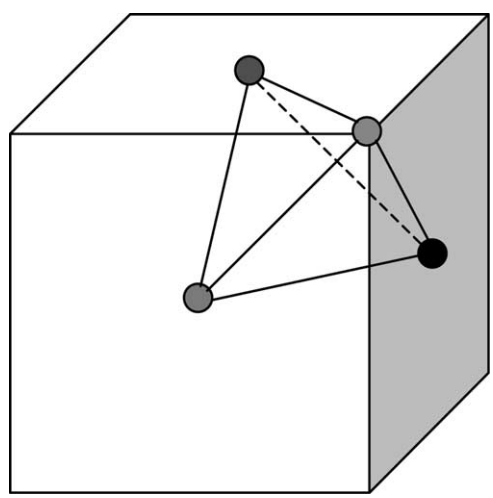

Fig. 1. A tetrahedron cluster taken from a face-centered cubic lattice containing four sites.

$$
\begin{aligned}
&\varepsilon_{AAAA} = {}^{o}G_{A}^{\psi} \\
&\varepsilon_{AAAB} = \varepsilon_{AABA} = \varepsilon_{ABAA} = \varepsilon_{BAAA} \\
&\quad = \varepsilon_{A_3B} = \frac{3}{4}{}^{o}G_{A}^{\psi} + \frac{1}{4}{}^{o}G_{B}^{\psi} + 3\omega_{AB} \\
&\varepsilon_{AABB} = \varepsilon_{ABAB} = \varepsilon_{ABBA} = \varepsilon_{BAAB} = \varepsilon_{BABA} \\
&\quad = \varepsilon_{BBAA} = \varepsilon_{A_2B_2} = \frac{1}{2}{}^{o}G_{A}^{\psi} + \frac{1}{2}{}^{o}G_{B}^{\psi} + 4\omega_{AB} \\
&\varepsilon_{ABBB} = \varepsilon_{BABB} = \varepsilon_{BBAB} = \varepsilon_{BBBA} \\
&\quad = \varepsilon_{AB_3} = \frac{1}{4}{}^{o}G_{A}^{\psi} + \frac{3}{4}{}^{o}G_{B}^{\psi} + 3\omega_{AB} \\
&\varepsilon_{BBBB} = {}^{o}G_{B}^{\psi}
\end{aligned}
\tag{12}
$$

where ε_{ijkl} represents the cluster energy of the cluster *ijkl*, ${}^{o}G_{p}^{\psi}$ is the Gibbs energy of the pure component p with structure ψ and ω_{AB} is the A-B pair exchange energy. The number of parameters required to be optimized is greatly reduced by doing this. In addition to the pair exchange energy, the other model parameters are the geometrical factor ξ and the L parameters in the configuration independent term as shown in Eq. (8).

The two ordered intermetallic phases, B2–NiAl and $D5_{13}$–Al_3Ni_2 have been described by a cluster energy model in the zeroth approximation (also known as the compound energy model [10]) as has been done in previous thermodynamic descriptions of this system [1–3]. The liquid phase has been described by a substitutional solution model, whilst the Al_3Ni and Al_3Ni_5 phases have been treated as stoichiometric compounds. The Gibbs energies of the pure elements given by Dinsdale [22] have been used in this study. The model parameters used for the f.c.c. phase as well as those for all the other phases are listed in Table 1. Note that since $NiAl_3$ ($L1_2$) is not a stable phase in this binary system, the relevant cluster energies have been given an arbitrary less negative value (−20 kJ/mol), as listed in Table 1. This value is very close to what has been calculated by using a 'first principles' approach, which is –21.754 kJ/mol [5].

4. Results and discussion

The model parameter optimizations and the property and phase diagram calculations have been carried out using the Winphad software package [23]. The calculated stable Ni–Al phase diagram is shown in Fig. 2, where it can be seen that the agreement between the calculated phase diagram and the experimental data [24–27] is excellent. Fig. 3 is an enlarged diagram of the region near the peritectic formation of the γ' from the liquid and the γ phases. The Al–Ni pair ordering is so strong that the γ' phase, the ordered state ($L1_2$), melts before there is a complete order/disorder transition.

As can be seen, the modified CSA is capable of calculating phase diagrams similar to those from other phenomenological calculations with the accuracy required for practical applications, which is not the case for those calculations [4–6] which use a 'first-principles'-CVM method. It also has the advantage over the zeroth approximation in that it takes short-range order into consideration which makes it more suitable for describing an order/disorder transition. These points can be illustrated by calculating the metastable phase diagram for the f.c.c. phases only. Fig. 4 shows such a diagram calculated by the model parameters developed in this study using the modified CSA model, while Fig. 5 is the one obtained from a 'first principles' calculation of the energies and the use of the CVM for the entropies [5].

These two figures have identical topologies with the $L1_2$ and $L1_0$ states being seen to be stable at low temperature and the disordered A1 stable at high temperatures. The miscibility gap on the Al-rich side of the $A1$ state is caused by an elastic instability as discussed by Carlsson and Sanchez [28] and Pasturel et al. [5]. The calculated phase transformation temperatures between $L1_2$ and $A1$, and $L1_0$ and $A1$ states are much higher in the 'first principles' calculation than those calculated in the present work, an indication that the 'first principles' calculated energy values are too large. A similar situation was found for the Cd-Mg system, where we found that a phenomenonlogical calculation in which the CSA was used, agreed with the experimental data much better than that from a 'first principles' energy calculation in which the CVM was used for the entropy [19].

It is for this reason that we believe the metastable f.c.c. phase diagram for the Ni–Al system calculated and shown in Fig. 4 is better than that

Table 1
The model parameters for the Ni–Al system developed by this study

Phase name	Model	Parameters
Liquid	Disorder solution (Al, Ni)	${}^0L^{liq}_{Al,Ni} = -197088 + 30.353 \cdot T$ ${}^1L^{liq}_{Al,Ni} = 5438$ ${}^2L^{liq}_{Al,Ni} = 64642 - 15 \cdot T$
B2	Compound energy (Al, Ni):(Ni, Va)	$G^{B2}_{Al:Ni} = {}^oG^{b.c.c.}_{Al} + {}^oG^{b.c.c.}_{Ni} - 150000 + 22.38 \cdot T$ $G^{B2}_{Al:Va} = {}^oG^{b.c.c.}_{Al} + 10000 - T$ $G^{B2}_{Ni:Ni} = 2 \cdot {}^oG^{b.c.c.}_{Ni}$ $G^{B2}_{Ni:Va} = {}^oG^{b.c.c.}_{Ni} + 162508 - 24.705 \cdot T$ ${}^0L^{B2}_{(Al,Ni):*} = -58360 + 12 \cdot T$ ${}^0L^{B2}_{*:(Ni,Va)} = -69948 + 36 \cdot T$
Al_3Ni_2	Compound energy 3(Al):2(Al,Ni):(Ni, Va)	$G^{Al:Ni}_{Al_3Al:Ni} = 5 \cdot G^{b.c.c.}_{Al} + G^{b.c.c.}_{Ni} - 40477 + 1.734 \cdot T$ $G^{Al:Ni}_{Al_3Al:Va} = 5 \cdot G^{b.c.c.}_{Al} + 30000 - 3 \cdot T$ $G^{Al:Ni}_{Al_3Ni:Ni} = 3 \cdot G^{b.c.c.}_{Al} + 3 \cdot G^{b.c.c.}_{Ni} - 420000 + 70 \cdot T$ $G^{Al:Ni}_{Al_3Ni:Va} = 3 \cdot G^{b.c.c.}_{Al} + 2 \cdot G^{b.c.c.}_{Ni} - 353500 + 65 \cdot T$ ${}^0L^{Al:Ni}_{Al_3(Al,Ni):*} = -40000$ ${}^0L^{Al:Ni}_{Al_3*:(Ni,Va)} = -23317$
Al_3Ni	Line compound 0.75(Al):0.25(Ni)	$G^{Al:Ni}_{Al_3Ni} = 0.75 \cdot {}^oG^{f.c.c.}_{Al} + 0.25 \cdot {}^oG^{f.c.c.}_{Ni} - 39200 + 4.5 \cdot T$
Al_3Ni_5	Line compound 0.375(Al):0.625(Ni)	$G^{Al:Ni}_{Al_3Ni_5} = 0.375 \cdot {}^oG^{f.c.c.}_{Al} + 0.625 \cdot {}^oG^{f.c.c.}_{Ni} - 53955 + 5 \cdot T$
f.c.c.	CSA 0.25(Al, Ni):0.25(Al, Ni):0.25(Al, Ni):0.25(Al, Ni)	$\omega_{Al:Ni} = -16615 + 1.6333 \cdot T$ $\varepsilon_{Ni_3Al} = 0.75 \cdot {}^oG^{f.c.c.}_{Ni} + 0.25 \cdot {}^oG^{f.c.c.}_{Al} + 3 \cdot \omega_{Al:Ni}$ $\varepsilon_{Ni_2Al_2} = 0.5 \cdot {}^oG^{f.c.c.}_{Ni} + 0.5 \cdot {}^oG^{f.c.c.}_{Al} + 4 \cdot \omega_{Al:Ni}$ $\varepsilon_{NiAl_3} = 0.25 \cdot {}^oG^{f.c.c.}_{Ni} + 0.75 \cdot {}^oG^{f.c.c.}_{Al} - 20000$ ${}^0L = 13500 + 10 \cdot T$ ${}^1L = -24460 + 7.484 \cdot T$ ${}^2L = 6600 - 4 \cdot T$ $\xi = 1.35$

shown in Fig. 5. The same metastable f.c.c. phase diagram has also been calculated using the parameters published by Huang and Chang [3] and Ansara et al. [2] and are shown in Figs. 6 and 7. Huang and Chang [3] treated γ, the disordered state ($A1$), and γ', the ordered state ($L1_2$) of the f.c.c. phase as two separate phases and described them by using two different models. The Gibbs energy of γ' in its disordered state is different from that of the γ phase, therefore, γ' cannot be disordered to γ based on their description. The metastable f.c.c. diagram shows equilibria between γ and disordered γ' at the upper right corner as shown in Fig. 6. Even though Ansara et al. [2] treated the γ and γ' as one phase using a two sublattice compound energy model, the order/disorder transition between γ' and γ cannot be correctly described as shown in Fig. 7 because short-range order was ignored in the model. This limitation is even more apparent when a four sublattice model is considered. As indicated by Ansara et al. [2], their two sublattice compound energy model used for the f.c.c. phase was simplified from a four sublattice format because only one ordered state ($L1_2$) was considered in their description. This makes it possible to adapt the parameters of their two-sublattice model to the four-sublattice case. A more complete f.c.c. metastable phase diagram is then calculated using the four sublattice compound energy model as shown in Fig. 8.

This metastable f.c.c. phase diagram is very similar to the classic one calculated by Shockley [29], who used a constant pairwise energy calculation in the same zeroth approximation. The slight difference between Fig. 8 and Shockley's diagram stems from the asymmetry of the cluster

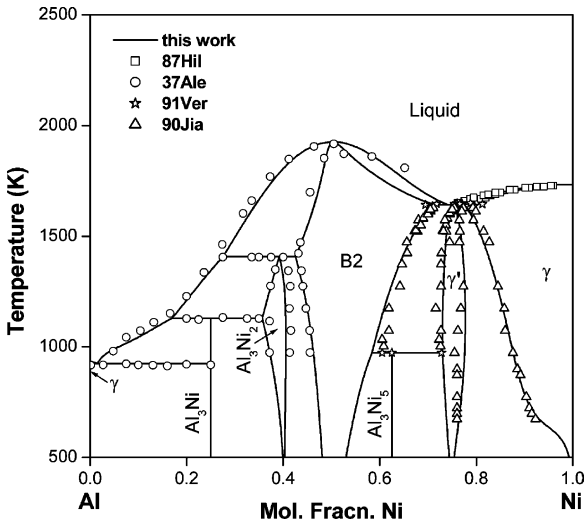

Fig. 2. Comparison between the calculated Ni–Al phase diagram and the experimental data: 87Hil [24], 37Ale [25], 91Ver [26], and 90Jia [27], excellent agreement is achieved.

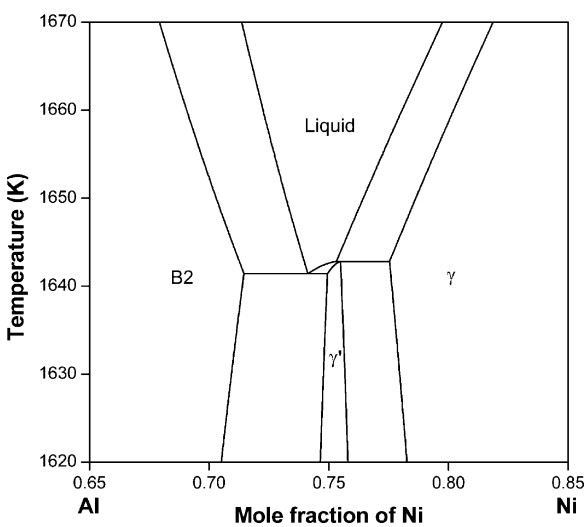

Fig. 3. Enlarged diagram of the region near the peritectic formation of the γ' from the liquid and the γ phases.

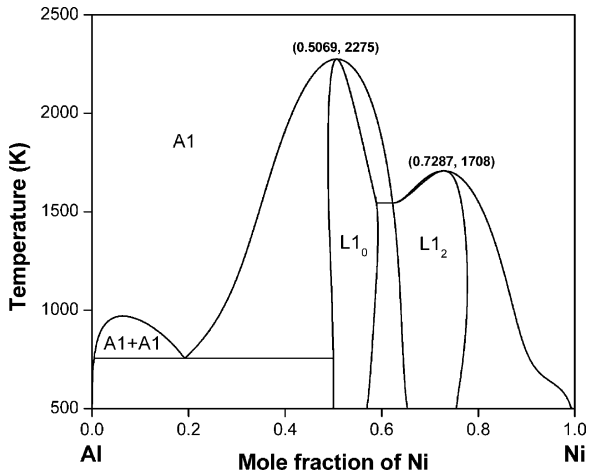

Fig. 4. The topology of the metastable f.c.c. phase diagram calculated by this work using the CSA model.

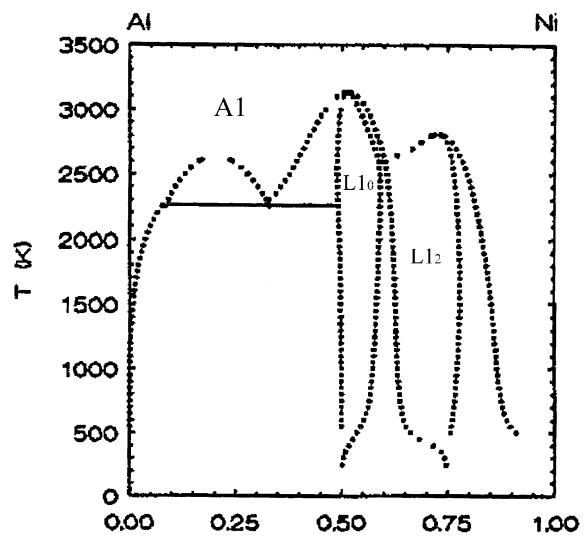

Fig. 5. The topology of the metastable f.c.c. phase diagram calculated by Pasturel et al. [5], using a 'first-principles'-CVM approach.

(compound) energies. The important point is that neither show the splitting in composition for the order/disorder transitions at the Ni_3Al, NiAl and $NiAl_3$ compositions. This is a result of the point approximation models not taking short range order into account.

Recently, however, Sundman et al. [30] and Kusoffsky and Sundman [31] have attempted to address this shortcoming of the compound energy model. In the first of the above papers, reciprocal sublattice L parameters were successful in splitting the order/disorder transitions for Au_3Cu, AuCu and $AuCu_3$ in the Au–Cu system. Higher order approximations achieve the same splitting by incorporating SRO. In the work of Sundman et al.

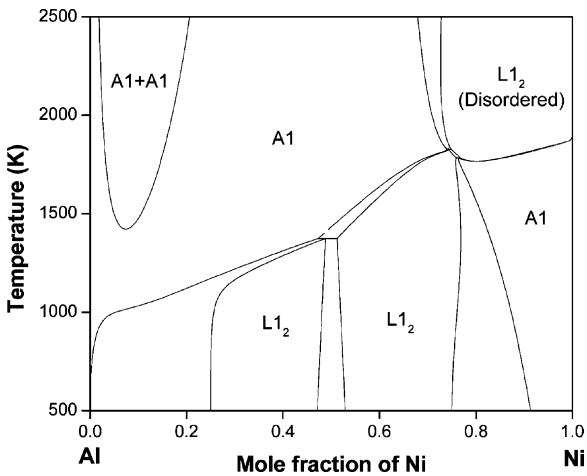

Fig. 6. The topology of the metastable f.c.c. phase diagram calculated by using the model parameters of Huang and Chang [3].

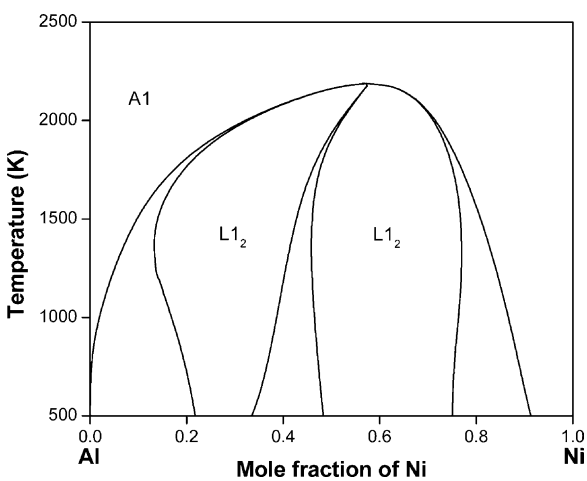

Fig. 7. The topology of the metastable f.c.c. phase diagram calculated by using the model parameters of Ansara et al. [2]. Two sublattice model.

[30] the configurational entropy is still given by the point approximation, i.e., there is no SRO. The total entropy of mixing is, however, modified by the use of a temperature co-efficient in the reciprocal sublattice L parameters and it is this which permits the ordered phase splitting to occur. The technique entails the use of extra model parameters in order to achieve the desired temperature/composition variation of the mixing entropy and it can only be descriptive. It could not

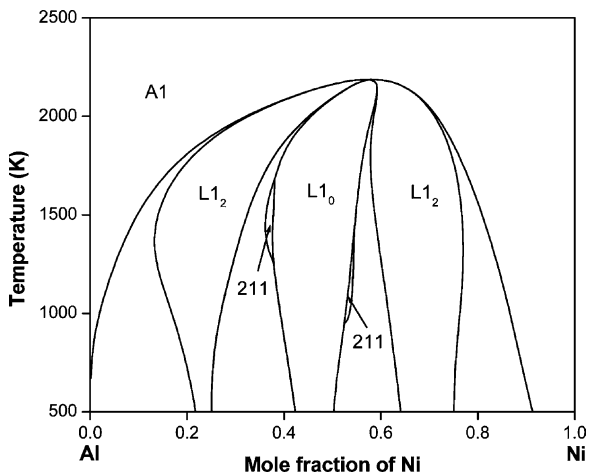

Fig. 8. The topology of the metastable f.c.c. phase diagram calculated by using the model parameters of Ansara et al. [2]. Four sublattice model.

be used in the calculation of a metastable f.c.c. phase diagram for the Al–Ni system, as was done in the case of Au–Cu, because the f.c.c. phase diagram, being metastable, is not known. In the second paper by Kusoffsky and Sundman [31] an attempt was made to reduce the number of independent variables in the CVM approximation by expressing the cluster probabilities in terms of their random values, as in the compound energy model, plus some internal parameters which are included in the free energy functional. It turned out that this worked satisfactorily for the disordered phase, giving results identical to those obtained with the CVM but with the same number of independent variables. The method failed, however, for ordered phases, where there are necessarily more cluster probabilities to consider.

In addition to the phase diagram, good agreement between the calculated and experimental results [32–35] is also found for the thermodynamic properties using the present description. This is illustrated in Fig. 9, which shows a comparison of calculated and experimental enthalpies of formation.

5. Conclusions

The CSA model has been used in obtaining a thermodynamic description of the f.c.c. phases in

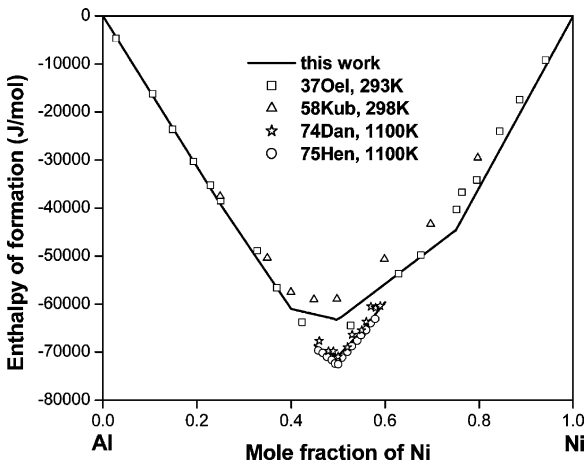

Fig. 9. Comparison between the calculated enthalpy of formation at 298 and 1100 K and the experimental data: 37Oel [32], 58Kub [33], 74Dan [34], and 75Hen [35], excellent agreement is achieved.

the Ni–Al system. The use of this model, where short-range order is taken into consideration, gives a superior description to those obtained previously where the zeroth approximation has been employed [1–3]. The calculated order/disorder transition between the γ and γ' phases, as well as the metastable f.c.c. phase diagram for this system, are much more plausible. Moreover, fewer model parameters than used in the previous studies [1–3] are required, whilst the calculated Ni–Al phase diagram and thermodynamic properties are as good as or better than those obtained in the previous work. The calculated Ni–Al phase diagram using the phenomenologically obtained energy parameters in conjunction with the modified CSA model reached the accuracy of practical application, which is not yet the case for those calculated from 'first principles' energy calculations in conjunction with the use of the CVM [4–6]. Even though not as physically sound as the CVM, the modified CSA model has the considerable advantage of computational simplicity over the CVM and, unlike the latter, seems very promising for the calculation of phase diagrams in multicomponent systems.

Acknowledgements

We should like to express our appreciation to a reviewer for his/her useful comments. We also wish to acknowledge financial support from an FRG on Maturation of Advanced Materials from NSF through the Ohio State University (Grant # NSF-DMR-0080766) for the effort at University of Wisconsin-Madison, and from the Air Force Research Laboratory, Wright-Patterson AFB, OH (Contract nos. F33615-99-C-5204 and F33615-00-C-5514) for the effort at CompuTherm, LLC.

References

[1] Du Y, Clavaguera N. J. Alloys Comp. 1996;237:20.
[2] Ansara I, Dupin N, Lukas HL, Sundman B. J. Alloys Comp. 1997;247:20.
[3] Huang W, Chang YA. Intermetallics 1998;6:487.
[4] Sigli C, Sanchez JM. Acta Metall. 1985;33:1097.
[5] Pasturel A, Colinet C, Paxton AT, van Schilfgaarde M. J. Phys. Condens. Matter. 1992;4:945.
[6] Lechermann F, Fahnle M. Phys. Stat. Sol. 2001;b224(2):R4.
[7] Bragg WL, Williams E. J. Proc. R. Soc. 1934;A145:699.
[8] Bragg WL, Williams E. J. Proc. R. Soc. 1935;A151:540.
[9] Kikuchi R. Phys. Rev. 1951;81:988.
[10] Sundman B, Agren J. J. Phys. Chem. Solids 1981;42:297.
[11] Oates WA, Zhang F, Chen SL, Chang YA. Physical Review B 1999;59(17):11221.
[12] Oates WA, Wenzl H. Scripta Mater. 1996;35:623.
[13] Fowler RH. Statistical mechanics., 2nd ed. Cambridge: Cambridge University Press, 1938.
[14] Yang CN. J. Chem. Phys 1945;13:66.
[15] Yang CN, Li Y. Chinese J. Phys. 1947;7:59.
[16] Li Y. J. Chem. Phys. 1949;17:447.
[17] Li Y. Phys. Rev. 1949;76:972.
[18] Zhang F, Oates WA, Chen SL, Chang YA. In: McNallan M, Opila E, editors. High temperature corrosion and materials chemistry III. The Electrochemical Society, 2001. p. 241.
[19] Zhang J, Oates WA, Zhang F, Chen S-L, Chou K-C, Chang YA. Intermetallics 2001;9(1):5.
[20] Oates WA, Wenzl H, Mohri T. CALPHAD 1996;20:37.
[21] Redlich O, Kister A. Ind. Eng. Chem. 1948;40:345.
[22] Dinsdale AT. CALPHAD 1991;15:317.
[23] Winphad, software package for binary phase diagram calculation and optimization, available at CompuTherm LLC, 437 S. Yellowstone Dr. Madison, WI 53719, USA.
[24] Hilpert K, Kobertz D, Venugopal V, Miller M, Gerads H, Bremer FJ, Nickel H. Z. Naturforsch.,A 1987;42A:1327.
[25] Alexander WO, Vaughan NB. J. Inst. Met. 1937;61:247.
[26] Verhoeven JD, Lee JH, Laabs FC, Lones LL. J. Phase Equil. 1991;12:15.

[27] Jia C C. Ph. D. thesis. Tohoku University, Japan, 1990.
[28] Carlsson AE, Sanchez JM. Solid State Commun. 1988;65:527.
[29] Shockley W. J. Chem. Phys. 1938;6:130.
[30] Sundman B, Fries SG, Oates WA. CALPHAD 1998;22:335.
[31] Kusoffsky A, Sundman B. Ber. Bunsenges. Phys. Chem. 1998;102:1111.
[32] Oelsen W, Middel W. Mitt. Kaiser-Wilhelm-Inst. Eisenforsch, Dusseldorf 1937;19:1.
[33] Kubaschewski O. Trans. Farady Soc. 1958;54:814.
[34] Dannohl H-D, Lukas HL. Z. Metallkd. 1974;65:642.
[35] Henig ET, Lukas HL. Z. Metallkd. 1975;66:98.